ISSN 1674-1056
http://cpb.iphy.ac.cn
http://iopscience.iop.org/cpb
中国物理 B
Chinese Physics
中国物理
Chinese Physics B

Two-dimensional transport and strong spin-orbit interaction in $SrMnSb_2$

Jiwei Ling(凌霁玮), Yanwen Liu(刘彦闻), Zhao Jin(金昭), Sha Huang(黄沙), Weiyi Wang(王伟懿), Cheng Zhang(张成), Xiang Yuan(袁翔), Shanshan Liu(刘姗姗), Enze Zhang(张恩泽), Ce Huang(黄策), Raman Sankar, Fang-Cheng Chou, Zhengcai Xia(夏正才), Faxian Xiu(修发贤)
Citation: Chin. Phys. B . 2018, 27(1): 017504. **doi:** 10.1088/1674-1056/27/1/017504

Journal homepage: http://cpb.iphy.ac.cn; http://iopscience.iop.org/cpb

What follows is a list of articles you may be interested in

Quantum spin Hall and quantum valley Hall effects in trilayer graphene and their topological structures

Majeed Ur Rehman, A A Abid
Chin. Phys. B . 2017, 26(12): 127304. **doi:** 10.1088/1674-1056/26/12/127304

Total ionizing radiation-induced read bit-errors in toggle magnetoresistive random-access memory devices

Yan Cui(崔岩), Ling Yang(杨玲), Teng Gao(高腾), Bo Li(李博), Jia-Jun Luo(罗家俊)
Chin. Phys. B . 2017, 26(8): 087501. **doi:** 10.1088/1674-1056/26/8/087501

Quantum anomalous Hall effect in real materials

Jiayong Zhang(张加永), Bao Zhao(赵宝), Tong Zhou(周通), Zhongqin Yang(杨中芹)
Chin. Phys. B . 2016, 25(11): 117308. **doi:** 10.1088/1674-1056/25/11/117308

Large linear magnetoresistance in a new Dirac material $BaMnBi_2$

Yi-Yan Wang(王义炎), Qiao-He Yu(郁巧鹤), Tian-Long Xia(夏天龙)
Chin. Phys. B . 2016, 25(10): 107503. **doi:** 10.1088/1674-1056/25/10/107503

Anomalous Hall effect in perpendicular CoFeB thin films

Zhu Tao
Chin. Phys. B . 2014, 23(4): 047504. **doi:** 10.1088/1674-1056/23/4/047504

RAPID COMMUNICATION

Two-dimensional transport and strong spin–orbit interaction in $SrMnSb_2$*

Jiwei Ling(凌霁玮)[1,2], Yanwen Liu(刘彦闻)[1,2], Zhao Jin(金昭)[3], Sha Huang(黄沙)[3], Weiyi Wang(王伟懿)[1,2], Cheng Zhang(张成)[1,2], Xiang Yuan(袁翔)[1,2], Shanshan Liu(刘姗姗)[1,2], Enze Zhang(张恩泽)[1,2], Ce Huang(黄策)[1,2], Raman Sankar[4], Fang-Cheng Chou[4], Zhengcai Xia(夏正才)[3,‡], and Faxian Xiu(修发贤)[1,2,5,†]

[1] *State Key Laboratory of Surface Physics and Department of Physics, Fudan University, Shanghai* 200433, *China*
[2] *Collaborative Innovation Center of Advanced Microstructures, Nanjing* 210093, *China*
[3] *Wuhan National High Magnetic Field Center, Huazhong University of Science and Technology, Wuhan* 430074, *China*
[4] *Center for Condensed Matter Science, "National" Taiwan University, Taipei* 11529, *Taiwan, China*
[5] *Institute for Nanoelectronic Devices and Quantum Computing, Fudan University, Shanghai* 200433, *China*

(Received 22 November 2017; published online 28 November 2017)

We have carried out magneto-transport measurements for single crystal $SrMnSb_2$. Clear Shubnikov–de Haas oscillations were resolved at relatively low magnetic field around 4 T, revealing a quasi-2D Fermi surface. We observed a development of quantized plateaus in Hall resistance (R_{xy}) at high pulsed fields up to 60 T. Due to the strong 2D confinement and layered properties of the samples, we interpreted the observation as bulk quantum Hall effect that is contributed by the parallel 2D conduction channels. Moreover, the spin degeneracy was lifted leading to Landau level splitting. The presence of anisotropic g factor and the formation of the oscillation beating pattern reveal a strong spin–orbit interaction in the $SrMnSb_2$ system.

Keywords: high field transport, spin–orbit interaction, anisotropic g factor, bulk quantum Hall effect

PACS: 75.47.–m, 75.70.Tj, 73.43.–f **DOI:** 10.1088/1674-1056/27/1/017504

1. Introduction

$SrMnSb_2$ is a member of widely studied ternary crystal family $AMnB_2$, A = Sr, Ca, Ba, Eu, Yb; B = Bi, Sb). This material group was reported to host quasi-2D Dirac fermions that possess outstanding physical properties.[1–13] Intriguingly, despite the theoretical prediction which suggests the absence of Dirac fermions in $SrMnSb_2$,[14] the nonstoichiometric coordinate $Sr_{1-y}Mn_{1-z}Sb_2$ ($y,z < 0.1$) was found to be magnetic topological semimetal.[12] Here we carried out the magneto-transport study for single crystal $SrMnSb_2$. A trivial Berry phase and a highly anisotropic Fermi surface were identified from Shubnikov–de Hass (SdH) oscillations. With the 60 T pulsed field, the sample was driven to the second Landau level. Accompanied by the minima in longitudinal resistance R_{xx}, the quantized plateaus were developed in Hall resistance R_{xy}. We interpreted the plateaus as the bulk quantum Hall effect that is attributed to the strong 2D confinement and layered structure of the material. Notably, the spin degeneracy is readily lifted at high fields, resulting in pronounced Zeeman splitting. Due to the strong spin–orbit interaction (SOI), the g factor calculated from the splitting is highly anisotropic. Moreover, the presence of the beating pattern in the SdH oscillations provides a direct evidence of the SOI splitting of the Fermi surface.

2. Experiment

2.1. Material characterizations

Our samples are nonstoichiometric single crystals with deficiencies in Sr and Mn. The sample providing the transport data has the specific composition of $Sr_{(0.88\pm0.02)}Mn_{(0.91\pm0.06)}Sb_2$ which is obtained by averaging four energy-dispersive x-ray spectroscopy (EDX) results. Despite the deficiency of the Sr and Mn elements, the bulk crystal exhibits a good crystalline quality as confirmed by the sharp diffraction peaks from the x-ray diffraction (XRD) spectrum (Fig. 1(b)). All the peak positions match well with those of the stoichiometric coordinate,[12] and the layer normal is along the a-axis. Data for additional samples are available in the supplementary materials.

2.2. SdH oscillations at low fields

Our samples were measured in a Hall bar geometry as illustrated in the inset of Fig. 1(c). A constant current was applied in the bc plane with a magnetic field along the a-axis (the out-of-plane direction). Figure 1(c) displays the temperature dependence of the resistivity (R–T curve) at zero field, which exhibits a metallic feature. Figure 1(d) shows the carrier density and mobility at different temperatures. Mobility up to

*Project supported by the National Key Research and Development Program of China (Grant No. 2017YFA0303302) and the National Natural Science Foundation of China (Grant Nos. 61322407, 11474058, and 61674040).

†Corresponding author. E-mail: Faxian@fudan.edu.cn
‡Corresponding author. E-mail: Xia9020@hust.edu.cn.cn

© 2018 Chinese Physical Society and IOP Publishing Ltd

6200 $cm^{-2}\cdot V^{-1}\cdot s^{-1}$ at 2.5 K was obtained from the Hall effect measurement. In the whole temperature range, the Hall signal shows positive slopes, indicating a hole-dominated transport behavior which is consistent with the previous report.[12] Notably, the electron carriers were reported to be dominant in $SrMnSb_2$ elsewhere.[15] The striking difference in the carrier type implies that $SrMnSb_2$ is a sensitive system that stringently relies on composition and growth details.

Typical magnetoresistance ($MR = [R(B) - R(0)]/R(0)$) is shown in Fig. 2(a). To explore the conduction channels' dimensionality, MR was measured at different angles. With the perpendicular geometry (the field direction is parallel to the a axis), the MR ratio almost reaches 200% at 2.5 K, which exceeds the previously reported giant MR in Dirac semimetals $CaMnBi_2$ (105%)[5] and $SrMnBi_2$ ($\sim$ 120%).[2] Moreover, clear SdH oscillations start to appear around 4 T. Subtracting the parabolic MR background resolves the evident SdH oscillations that persist beyond 20 K. Only one main frequency was observed in fast Fourier transform (FFT) spectrum at each angle in the field range of 0–9 T. The oscillation frequency is associated with the external cross-sectional area of the Fermi surface (A_F). For a 2D Fermi surface, the cross section has an angular dependence following $A_F(\theta) = A_0/|\cos(\theta)|$. The angle θ is defined as the angle between the magnetic field and the normal of the bc plane. As displayed in Fig. 2(b), the angular dependence of the frequency follows the cosine law (the red dashed curve). The quasi-cosine behavior of the frequency indicates a highly anisotropic Fermi surface. Similar oscillation analysis was carried out for the temperature-dependent MR in Fig. 2(c). For the oscillation at 2.5 K, the Fourier spectrum reveals a single frequency of $F = 74.6$ T (the inset of Fig. 2(c)). Oscillations at other temperatures also reveal the same frequency since there was no apparent peak shift. Deducing from the Onsager relation $F = \left(\frac{\Phi_0}{2\pi^2}\right) A_F$ (Φ_0 is the flux quantum), the frequency of 74.6 T corresponds to the external cross-sectional area of the Fermi surface $A_F = 0.71$ nm^{-2}. This area is just slightly larger than that of the nonstoichiometric sample which hosts the relativistic fermions.[12]

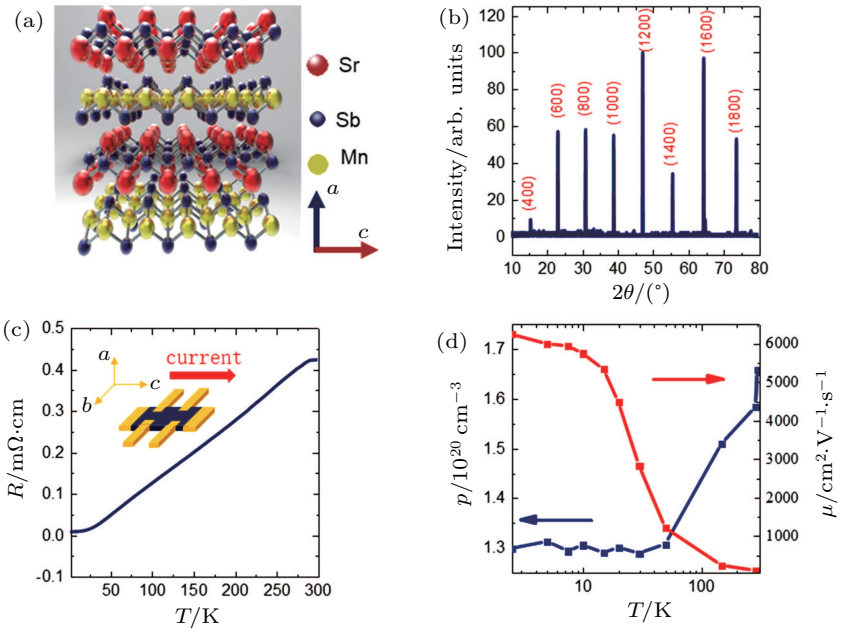


Fig. 1. (color online) Characterization of $Sr_{1-x}Mn_{1-y}Sb_2$. (a) A schematic drawing of $SrMnSb_2$ crystal structure. Single crystal $SrMnSb_2$ is composed of two formula layers (SrSb and MnSb), stacking along the a axis. (b) X-ray diffraction pattern of $Sr_{0.88}Mn_{0.91}Sb_2$ on the (00l) plane. The XRD pattern peaks of our sample match well with the stoichiometric coordinate. (c) The temperature dependence of in-plane resistivity. A constant current was applied within the bc plane. The inset shows the geometry of Hall bar. (d) The carrier density and mobility at different temperatures. The mobility of the sample exceeds 6200 $cm^2\cdot V^{-1}\cdot s^{-1}$ at 2.5 K.

We performed the fitting of the temperature-dependent oscillation amplitudes to the Lifshits–Kosevich formula:[16]

$$\Delta R_{xx} \propto R_T R_D R_s \cos\left[2\pi\left(\frac{F}{B}\right) + \phi\right],$$

where

$$R_T \propto \frac{2\pi^2 k_B T m^*/\hbar eB}{\sinh(2\pi^2 k_B T m^*/\hbar eB)},$$

$$R_D \propto \exp\left[-\left(\frac{\pi m^*}{eB\tau_Q}\right)\right],$$

$$R_s = \cos\left(\frac{\pi g m^*}{2m_0}\right).$$

Identifying the oscillation amplitudes at different temperatures at one specific magnetic field strength and fitting the set of data to the R_T formula enable the extraction of the effective mass. The fitting yields an effective mass $m^* = (0.126 \pm 0.003)m_0$, where m_0 is the bare electron mass. This value is larger than the conventional Dirac semimetal system, such as Cd_3As_2 ($0.044m_0$),[17] but smaller than those of Dirac cousins

$SrMnBi_2$ ($0.29m_0$)[2] and $CaMnBi_2$ ($0.32m_0$).[5]

The expression of Dingle temperature is $T_D = \frac{\hbar}{2\pi\tau_Q k_B}$, where τ_Q is the quantum lifetime of carries due to scattering. It can be obtained from the slope of the linear fitting of $\ln[D] \sim 1/B$, $D = \Delta R B \sinh\left(\frac{2\pi^2 k_B T m^*}{\hbar e B}\right)$. As shown in Fig. 2(e), the Dingle temperature is found to be 15 K at $T = 2.5$ K. Then we extract the carrier lifetime $\tau_Q = 8.18\times10^{-14}$ s. The quantum lifetime τ_Q (also known as the single-particle lifetime) and the transport lifetime are two important time scales. It is widely accepted[18] that the ratio $R_\tau \equiv \frac{\tau_t}{\tau_Q}$ is an indication of the dominant scattering mechanism since the quantum lifetime τ_Q obtained from SdH oscillations measures the collision events at all directions while τ_t obtained from the conductivity ($\tau_t = \frac{\mu_e m^*}{e}$) counts the collision events in only particular direction.[18] In our trivial $SrMnSb_2$ system, τ_t is 4.44×10^{-13} s, giving $R_\tau = 5.42$, which is in the conventional case that the transport lifetime is regarded as the same order as the quantum lifetime. Commonly, larger ratio is expected in topological system, since the large ratio between the two time scales is usually associated with the suppression of backscattering that originates from the chiral nature in topological semimetal systems.[19] Besides the 2DEG systems with a factor of 10–100,[18,20–22] the large R_τ was reported in Weyl semimetal TaAs[23] and in topological semimetal LaSb with an extraordinary large value reaching 10^4.[24]

The corresponding mobility obtained from the quantum lifetime is $\mu = \frac{e\tau_Q}{m^*} \sim 1125$ cm^2/Vs, which is significantly larger than that of $SrMnBi_2$.[2] It is remarkable that the sample's physical properties are comparable with its Dirac cousins, requiring us to attain more information on sample's relativistic properties. Therefore, we calculated the Berry phase accumulated along cyclotron orbits.

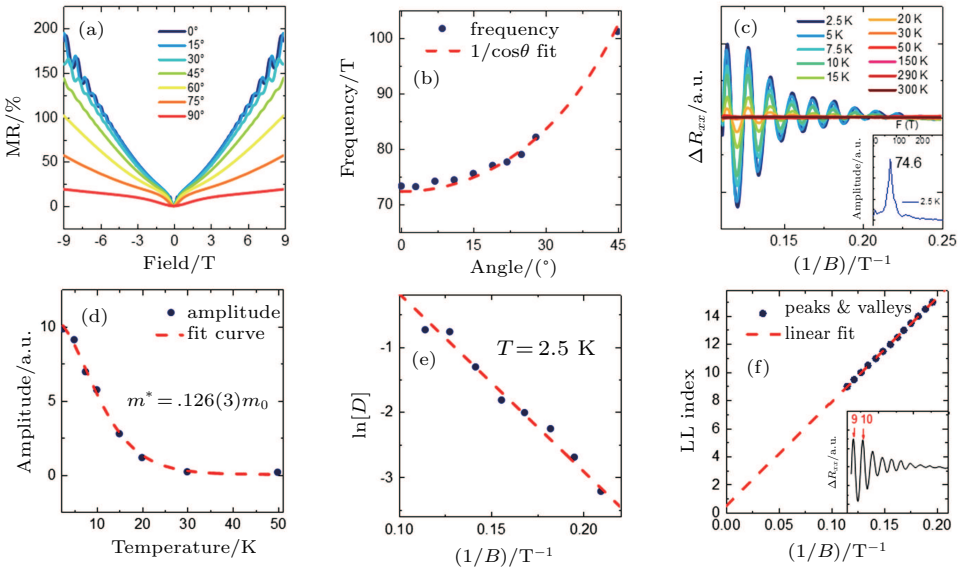


Fig. 2. (color online) SdH oscillations at low fields. (a) The magneto-resistance ratio $((R(B)-R(0))/R(0))$ at different angles. The angle of magnetic field is defined as the angle between the magnetic field and the normal of the *bc* plane (zero degree means that the magnetic field is perpendicular to the *bc* plane). The maximum MR ratio is approximately 200%. Clear SdH oscillations persist beyond 45°. (b) The angular dependence of the oscillation frequency, following the cosine law $F(\theta) = F_0/|\cos(\theta)|$. The red dashed curve indicates the cosine fitting. (c) SdH oscillations at different temperatures. ΔR_{xx} were obtained by subtracting a parabolic background. Inset: Fourier transform of the oscillations at 2.5 K, revealing a single frequency $F = 74.6$ T. (d) The Lifshitz–Kosevich formula fitting to the oscillation amplitudes at different temperatures. The fit yields the cyclotron effective mass $m^* = 0.126 \pm 0.003 m_0$, where m_0 is the bare electron mass. (e) Dingle plot. The oscillation amplitude at 2.5 K decays exponentially. The Dinge temperature fitting yields the Dingle temperature of 15 K. The quantum lifetime obtained is 4.44×10^{-13} s. (f) Landau index plot. Inset: integers correspond to the valleys in the conductance spectrum. All the data align well on a straight line. The red dashed line is the linear fit using $n = \frac{F}{B} + \phi$. The intercept 0.55 ± 0.05 corresponds to a trivial Berry phase either for 2D or 3D system.

In the Lifshitz–Kosevich (LK) formula,[16] ΔR_{xx} is proportional to $\cos[2\pi(\frac{F}{B}) + \phi]$, where F, B, and Φ stand for frequency, magnetic field, and phase shift, respectively. It is widely believed that in a Dirac system, the linear dispersion band contributes an extra π Berry phase, which leads to a different phase shifts in 2D (1/8) and 3D (0) systems.[25] To avoid the obstacles in carrying out a complete fitting for the oscillation pattern by the LK formula, an alternative approach is through the Landau fan diagram. In the Landau fan diagram in which the inverse magnetic field $(1/B)$ is set as x-axis and integer n as y-axis, the position of peaks and valleys will fall on a straight line. Then F and ϕ can be extracted from the linear fit using $N = F/B + \phi$.[25] It is worth to mention that due to the complexity of the Landau level quantization in 3D semimetal systems, the assignment of the integer index is different from the cases of the topological insulator and graphene.[25] We follow the rule that is suggested by Wang[25] to index the extrema, in which the Landau level integers are assigned to the peaks in resistivity oscillation. The slope of the linear fitting corresponds to the oscillation frequency. The

value 74.0 ± 0.3 T is consistent with the FFT result. A phase shift $\phi = 0.55 \pm 0.05$ (Fig. 2(f)) was obtained, which corresponds to a trivial Berry phase.

The trivial Berry phase was suggested by the theoretical calculation.[14] As illustrated in Fig. 1(a), the crystal structure of $SrMnSb_2$ is similar to its cousin material $SrMnBi_2$, consisting of a periodic arrangement of Mn–Sb and Sr–Sb layers along the a axis, but with an orthorhombic distortion. The distortion in Sb layer dictates the symmetry and is responsible for the absence of the Dirac fermion. Practically, the composition of our sample has a small deviation from the stoichiometry, which is $Sr_{(0.88\pm0.02)}Mn_{(0.91\pm0.06)}Sb_2$, while the crystal structure remains unchanged compared to the stoichiometric sample as evidenced by the XRD pattern. Thus, we consider that the chemical deficiency is not likely to significantly modify the crystal symmetry and introduce Dirac points in our sample's band structure.

2.3. Bulk quantum Hall effect

To investigate the transport behavior when approaching the quantum limit, we applied a pulsed magnetic field up to 60 T. We observed the developing of quantized plateaus in R_{xy}. Each plateau position is aligned with the minima of R_{xx} as shown in Fig. 3(a). We interpreted the quantized feature as the multilayered quantum Hall effect arising from the stacked 2D conduction channels. Due to the weak interlayer interaction between unit layers and the strong 2D confinement revealed in the transport, the bulk sample behaves like a stacked system forming by many parallel 2D channels. The bulk quantum Hall effect has been reported in highly-doped topological insulator Bi_2Se_3,[26] Dirac semimetal $ZrTe_5$,[27] η-M_4O_{11},[28] and Bechgaard salts.[29–31] The quantized Hall resistance takes value $\sim \frac{e^2}{h}NZ$, where Z is the number of stacked quantum layers, and N is the Landau index. Figure 3(b) displays $1/R_{xy}$ scaled with Z as a function of N. The sample thickness is around 80 μm, the value of lattice parameter c calculated from XRD data is 23.12 ± 0.02 Å (the uncertainty comes from the standard deviation across the measured peaks), and each unit layer contains two van der Waals layers Sr–Sb and Mn–Sb. The inset shows that the scaled $1/R_{xy}$ falls on a straight line. The linear fit gives a slope of $(3.75 \pm 0.10) \times 10^{-5}$, which indicates a deviation of 3% to the value of $e^2/h = 3.874 \times 10^{-5}$. The error could come from the estimation of sample thickness and the deficiency-leading non-ideal current paths. The highly linear relation between the $1/R_{xy}$ value and the index shows an excellent quantization coming from the multilayered quantum Hall effect.

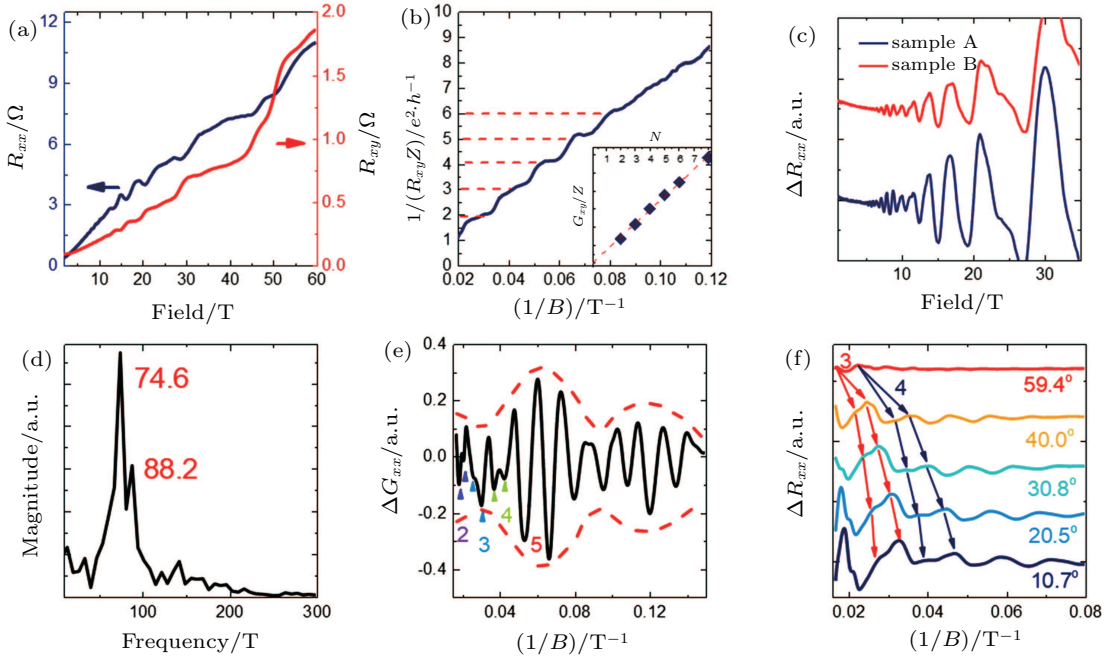


Fig. 3. (color online) Pulsed high field experiments. (a) Magnetoresistance (R_{xx}) and Hall resistance (R_{xy}) as functions of the perpendicular field along the a axis. The data is presented at 4.2 K. (b) Nearly quantized plateau in G_{xy} divided by the number Z as a function of $1/B$. Adjacent LLs are separated by e^2/h. Inset: normalized G_{xy} of each Landau level aligns in a straight line. Red dashed line is the linear fitting, yielding a slope of $3.75 \pm 0.10 \times 10^{-5}$ with 3% deviation from the standard value $e^2/h = 3.874 \times 10^{-5}$. (c) Oscillatory beating patterns were developed in sample 1 and sample 2. The first node position is around 10 T. (d) Peak splitting in the FFT transform spectrum of high field SdH oscillations of sample 1. The two frequencies are 74.6 T and 88.2 T respectively, indicating two Fermi surfaces differing 18% in cross-section areas. (e) Conductivity oscillation in $1/B$ scale at 4.2 K with $\theta = 0°$. Pulsed field of 60 T drove sample to the second Landau level. Pronounced Zeeman splitting was observed as labeled on the plot. An oscillatory beating pattern can be observed. The red dashed line is for guiding eyes. (f) Angular dependence of the Zeeman splitting spacing. Red and navy arrows show the splitting spacing change of the 3th and 4th Landau levels.

2.4. SOI induced beating and anisotropic g factor

Meanwhile, the field-dependent resistance evolves into a beating pattern with the first beating node positioned at 10 T. The beating pattern indicates the existence of two frequencies. Accordingly, the Fourier transform analysis of the resistance oscillation engenders a double-peak spectrum (Fig. 3(d)). The first frequency 74.6 T corresponds to the frequency appeared at low fields. The other frequency is 88.2 T. The two frequencies stand for two A_F differing by 18%, which means that there are two sets of Landau levels with comparable carrier density and cross-section area.

With the magnetic field strength up to 60 T, we can probe the transport channels with relatively low mobility. It is possible that an additional channel with lower mobility contributes to the beating feature. According to the SdH oscillations, the Fermi level lies around 138 meV below the top of the valence band where a small pocket located at Y could be involved in the transport. However, the difference between the cross-section areas of pocket at Y and Γ is remarkable and tends to rule out the two-band origin of the beating oscillation.

Zeeman splitting only produces two identical sets of sublevels along the field direction, so that the interference between the two sets of sublevels will not give rise to the beating pattern. On the other hand, a large spin orbit interaction often causes electronic band structure splitting and can manifest itself as a beating behavior in the SdH oscillations.[32–34] There are two types of spin–orbit interaction: Rashba type and Dresselhaus type. Rashba terms appear in the systems lacking of interface inversion symmetry, while Dresselhaus effect is considered in bulk inversion asymmetry crystals.[35] The distorted Sb atom net intrinsically breaks the inversion symmetry in $SrMnSb_2$ along the a crystallographic axis. Meanwhile, Sb atom is relatively heavy, thus sizable spin–orbit coupling should be expected in the sample.[35] Besides, Rashba terms usually play significant roles in 2D electron gas systems[32,33,36] and also manifest in topological insulator surface states.[37] For a trivial parabolic band, the Fermi energy is proportional to carrier density. The 18% splitting in density can be translated into 18% splitting in the Fermi energy, corresponding to the SOI splitting on the order of 20 meV.[34] Although the dominated SOI type requires more detailed work to determine, the presence of splitting in SdH oscillation frequency is a direct manifestation of the SOI splitting in the Fermi surface.

In the presence of the strong SOI, spins with different orientations are mixed in the Zeeman sublevels, and give rise to variations in g factor from the pure Zeeman splitting. It is noticeable that the magnetic field above 22 T lifts the Zeeman splitting as shown in Fig. 3(e), where pronounced splitting peaks and valleys were resolved in the conductance oscillation curves. It is known that Zeeman splitting is subjected to the total external magnetic field and it should be independent of the field direction. However, we observe the angular-dependent oscillations in the high field regime, as displayed in Fig. 3(f). The splitting spacing in our sample shows an obviously angular dependence. The g factor calculated at 10 degree is 5.0 which differs from the value at 40 degree (3.5) by 30%. An angular-dependent Zeeman splitting can be developed when SOI is involved by which the external field can induce exchange interaction. Any exchange splitting can be decomposed into the orbital independent and dependent part.[38] The former one corresponds to the isotropic Zeeman splitting part, while the latter one is highly sensitive to the field's direction, giving rise to a highly anisotropic g factor.[39] The anisotropic g factor is discovered in many 2D hole systems[40] as well as in the interface of heterostructrues,[41–44] where Rashba-type SOI usually dominates. Similar g factor variation is also discovered in materials that exhibit highly anisotropic Fermi surface, such as $ZrTe_5$.[27] The anisotropic g factor provides another unambiguous evidence of the SOI in $SrMnSb_2$.

3. Conclusion and perspectives

In conclusion, we carried out magneto-transport experiments for single crystal $SrMnSb_2$. Trivial hole-like carriers dominate in the transport measurements, which implies the composition sensitivity of sample's band structure. We suggest a fine-tuning composition experiments by molecular-beam epitaxy to explore sample's topological properties evolution. Angular dependent SdH oscillations reveal a quasi-2D Fermi surface. The strong 2D confinement also manifest itself in high field Hall signals where quantized plateaus are aligned with the minima in resistance oscillation. We interpret this behavior to the stacked parallel 2D conduction channels. Besides, the pulsed high field up to 60 T lifts sample's spin degeneracy leading to the pronounced Zeeman splitting. Anisotropic g factor and the development of the beating oscillation pattern reveal a significant spin–orbit interaction in the system. The outstanding transport properties, together with its layered nature and strong spin–orbit interaction render $SrMnSb_2$ to be an attractive candidate in the spintronics field.

Acknowledgments

Measurements in pulsed magnetic field were performed at Wuhan National High Magnetic Field Center, China. F. X. acknowledges the support from the open project of Wuhan National High Magnetic Field Center (#PHMFF2015003). J. L. sincerely thanks Wei Wang and Yiqing Hao for discussions.

References

[1] Wang J K, Zhao L L, Yin Q, Kotliar G, Kim M S, Aronson M C and Morosan E 2011 *Phys. Rev. B* **84** 064428

[2] Park J, Lee G, Wolff-Fabris F, Koh Y Y, Eom M J, Kim Y K, Farhan M A, Jo Y J, Kim C, Shim J H and Kim J S 2011 *Phys. Rev. Lett.* **107** 126402

[3] Wang K, Graf D, Lei H, Tozer S W and Petrovic C 2011 *Phys. Rev. B* **84** 220401

[4] Wang K, Graf D, Wang L, Lei H, Tozer S W and Petrovic C 2012 *Phys. Rev. B* **85** 041101

[5] He J B, Wang D M and Chen G F 2012 *Appl. Phys. Lett.* **100** 112405

[6] Lee G, Farhan M A, Kim J S and Shim J H 2013 *Phys. Rev. B* **87** 245104

[7] Feng Y, Wang Z, Chen C, Shi Y, Xie Z, Yi H, Liang A, He S, He J, Peng Y, Liu X, Liu Y, Zhao L, Liu G, Dong X, Zhang J, Chen C, Xu Z, Dai X, Fang Z and Zhou X J 2014 arXiv:1312.0227

[8] May A F, McGuire M A and Sales B C 2014 *Phys. Rev. B* **90** 075109

[9] Guo Y F, Princep A J, Zhang X, Manuel P, Khalyavin D, Mazin I I, Shi Y G and Boothroyd A T 2014 *Phys. Rev. B* **90** 075120

[10] Jo Y J, Park J, Lee G, Eom M J, Choi E S, Shim J H, Kang W and Kim J S 2014 *Phys. Rev. Lett.* **113** 156602

[11] Masuda H, Sakai H, Tokunaga M, Yamasaki Y, Miyake A, Shiogai J, Nakamura S, Awaji S, Tsukazaki A, Nakao H, Murakami Y, Arima T, Tokura Y and Ishiwata S 2016 *Sci. Adv.* **2** e1501117

[12] Liu J Y, Hu J, Zhang Q, Graf D, Cao H B, Radmanesh S M A, Adams D J, Zhu Y L, Cheng G F, Liu X, Phelan W A, Wei J, Jaime M, Balakirev F, Tennant D A, DiTusa J F, Chiorescu I, Spinu L and Mao Z Q 2017 *Nat. Mater.* **16** 905

[13] Wang A, Graf D, Wu L, Wang K, Bozin E, Zhu Y and Petrovic C 2016 *Phys. Rev. B* **94** 125118

[14] Farhan M A, Lee G and Shim J H 2014 *J. Phys.: Condens. Mat.* **26** 042201

[15] Park H J, Sandilands L J, You J S, Ji H S, Sohn C H, Han J W, Moon S J, Kim K W, Shim J H, Kim J S and Noh T W 2016 *Phys. Rev. B* **93** 205122

[16] Shoenberg D 2009 *Magnetic Oscillation in Metals* (Cambridge, UK: Cambridge University Press)

[17] He L P, Hong X C, Dong J K, Pan J, Zhang Z, Zhang J and Li S Y 2014 *Phys. Rev. Lett.* **113** 246402

[18] Harrang J P, Higgins R J, Goodall R K, Jay P R, Laviron M and Delescluse P 1985 *Phys. Rev. B* **32** 8126

[19] Jiang Q D, Jiang H, Liu H, Sun Q F and Xie X C 2016 *Phys. Rev. B* **93** 195165

[20] Das Sarma S and Stern F 1985 *Phys. Rev. B* **32** 8442

[21] Coleridge P T 1991 *Phys. Rev. B* **44** 3793

[22] MacLeod S J, Chan K, Martin T P, Hamilton A R, See A, Micolich A P, Aagesen M and Lindelof P E 2009 *Phys. Rev. B* **80** 035310

[23] Zhang C L, Yuan Z, Jiang Q-D, Tong B, Zhang C, Xie X C and Jia S 2017 *Phys. Rev. B* **95** 085202

[24] Tafti F F, Gibson Q D, Kushwaha S K, Haldolaarachchige N and Cava R J 2016 *Nat. Phys.* **12** 272

[25] Wang C M, Lu H Z and Shen S Q 2016 *Phys. Rev. Lett.* **117** 077201

[26] Cao H, Tian J, Ireneusz M, Shen T, Hu J, Qiao S and Chen Y P 2012 *Phys. Rev. Lett.* **108** 216803

[27] Liu Y, Yuan X, Zhang C, Jin Z, Narayan A, Luo C, Chen Z, Yang L, Zou J, Wu X, Sanvito S, Xia Z, Li L, Wang Z and Xiu F 2016 *Nat. Commun.* **7** 12516

[28] Hill S, Uji S, Takashita M, Terakura C, Terashima T, Aoki H, Brooks J S, Fisk Z and Sarrao J 1998 *Phys. Rev. B* **58** 10778

[29] Balicas L, Kriza G and Williams F I B 1995 *Phys. Rev. Lett.* **75** 2000

[30] Cooper J R, Kang W, Auban P, Montambaux G, Jérome D and Bechgaard K 1989 *Phys. Rev. Lett.* **63** 1984

[31] Hannahs S T, Brooks J S, Kang W, Chiang L Y and Chaikin P M 1989 *Phys. Rev. Lett.* **63** 1988

[32] Wang X F, Vasilopoulos P and Peeters F M 2005 *Phys. Rev. B* **71** 125301

[33] Heida J P, van Wees B J, Kuipers J J, Klapwijk T M and Borghs G 1998 *Phys. Rev. B* **57** 11911

[34] Wang Z, Ki D K, Khoo J Y, Mauro D, Berger H, Levitov L S and Morpurgo A F 2016 *Phys. Rev. X* **6** 041020

[35] Gambardella P and Miron I M 2011 *Philos. Trans. R. Soc. Lond. Math. Phys. Eng. Sci.* **369** 3175

[36] Grundler D 2000 *Phys. Rev. Lett.* **84** 6074

[37] King P D C, Hatch R C, Bianchi M, Ovsyannikov R, Lupulescu C, Landolt G, Slomski B, Dil J H, Guan D, Mi J L, Rienks E D L, Fink J, Lindblad A, Svensson S, Bao S, Balakrishnan G, Iversen B B, Osterwalder J, Eberhardt W, Baumberger F and Hofmann Ph. 2011 *Phys. Rev. Lett.* **107** 096802

[38] Wang Z, Sun Y, Chen X Q, Cesare F, Xu G, Weng H, Dai X and Fang Z 2012 *Phys. Rev. B* **85** 195320

[39] Winkler R, Papadakis S J, De Poortere E P and Shayegan M 2000 *Phys. Rev. Lett.* **85** 4574

[40] Zhao Y, Liu H, Zhang C, Wang H, Wang J, Lin Z, Xing Y, Lu H, Liu J, Wang Y, Brombosz Scott M, Xiao Z, Jia S, Xie X C and Wang J 2015 *Phys. Rev. X* **5** 031037

[41] Petta J R and Ralph D C 2002 *Phys. Rev. Lett.* **89** 156802

[42] Destefani C F and Ulloa Sergio E 2005 *Phys. Rev. B* **71** 161303

[43] Koduvayur S P, Rokhinson L P, Tsui D C, Pfeiffer L N and West K W 2008 *Phys. Rev. Lett.* **100** 126401

[44] Robert Zielke, Franziska Maier and Daniel Loss 2014 *Phys. Rev. B* **89** 115438